Abundance of Hard-Hexagon Crystals in the Quantum Pyrochlore Antiferromagnet

Robin Schäfer[*], Benedikt Placke[†], Owen Benton[‡], and Roderich Moessner[§]

Max Planck Institute for the Physics of Complex Systems, Noethnitzer Strasse 38, 01187 Dresden, Germany

We propose a simple family of valence-bond crystals as potential ground states of the $S = 1/2$ and $S = 1$ Heisenberg antiferromagnet on the pyrochlore lattice. Exponentially numerous in the linear size of the system, these can be visualized as hard-hexagon coverings, with each hexagon representing a resonating valence-bond ring. This ensemble spontaneously breaks rotation, inversion, and translation symmetries. A simple, yet accurate, variational wave function allows a precise determination of the energy, confirmed by the density matrix renormalization group and numerical linked cluster expansion, and extended by an analysis of excited states. The identification of the origin of the stability indicates applicability to a broad class of frustrated lattices, which we demonstrate for the checkerboard and ruby lattices. Our work suggests a perspective on such quantum magnets, in which *unfrustrated* motifs are effectively uncoupled by the frustration of their interactions.

The propensity of frustrated quantum magnets to host exotic ground states makes them a rewarding target for study. For several of the most prominent models, however, it has proved difficult to come to a consensus about the exact nature of the ground state [1–40]. This is particularly true for frustrated isotropic Heisenberg models with low spin $S \leq 1$ in dimension $d > 1$, for which approximate analytical methods are generally uncontrolled and numerical studies are challenging. To improve the situation requires simple yet reliable heuristics, by which we can understand not just which state is the ground state but also whence it derives its stability.

Amongst frustrated lattices, the pyrochlore lattice—a network of corner-sharing tetrahedra [Fig. 1(a)]—is a particularly tricky case. Several proposals have been made for the ground state of the nearest neighbor pyrochlore Heisenberg model for $S = 1/2$ including various forms of quantum spin liquid (QSL) [27–32], valence-bond solids [33–39,41,42], or the possibility that it lies on a phase boundary between different QSLs [40]. Two recent numerical studies found evidence of inversion symmetry breaking [37,38], consistent with one of the earliest proposals [35].

In this Letter, we propose a family of valence-bond crystal states generated from hard (nonoverlapping) hexagon coverings of the pyrochlore lattice [43] shown in Fig. 1(a). A one-parameter variational wave function

describing these states achieves an energy equal to the best-known proposals to date to within numerical uncertainties. The hard-hexagon crystal states are exponentially numerous in the linear system size, demonstrating the abundance of competing low-energy states. The difficulty in arriving at a consensus over the ground state is likely in considerable part due to the presence of so many competing states with barely distinguishable energies.
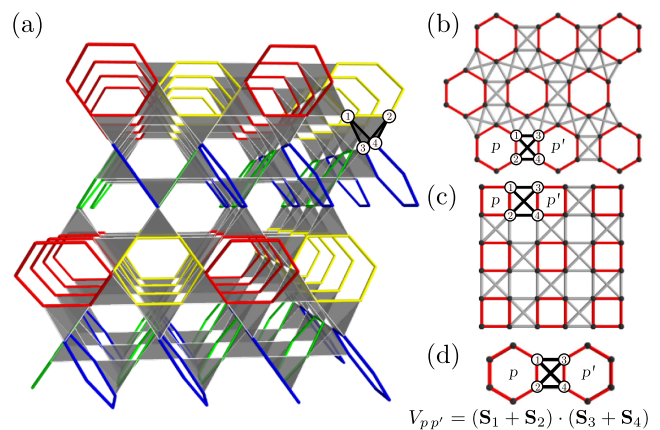

FIG. 1. Lattices composed of unfrustrated motifs coupled via a quartet of frustrated bonds. (a) A hard-hexagon tiling [43] of the pyrochlore showing $2 \times 2 \times 2$ unit cells, each containing 48 sites. The different colors represent the four different orientations of hexagons. (b) The ruby lattice with additional frustrated couplings exhibiting a unique hard-hexagon tiling. (c) The checkerboard lattice shows one of two possible tilings with unfrustrated squares. (d) Illustration of doubly frustrated interactions between motifs: two pairs of antiferromagnetically correlated spins are symmetrically coupled, making the interaction effectively a product of two small terms.

$$V_{pp'} = (\mathbf{S}_1 + \mathbf{S}_2) \cdot (\mathbf{S}_3 + \mathbf{S}_4)$$
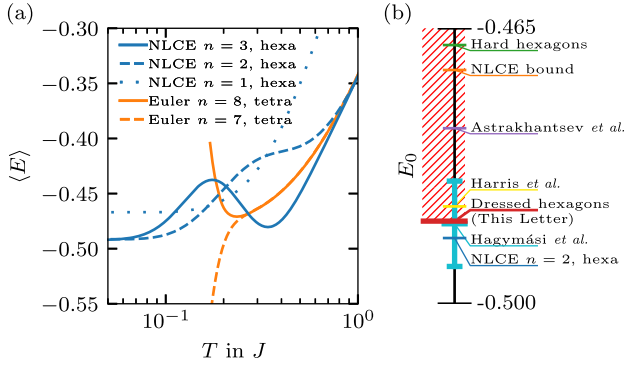
FIG. 2. (a) Energy per site at finite temperature for the pyrochlore $S = 1/2$ and $J = 1$. The orange curves are showing a tetrahedron-based NLCE expansion up to eighth order [59], which defines an upper limit for the ground-state energy. The blue curves show the NLCE expansion based on the hexagons. Euler refers to a resummation algorithm extending the convergence down to lower temperatures [59]. (b) Different estimates for the ground-state energy per site: bare hard hexagons (ground state of H_0), upper bound obtained by the converged tetrahedron expansion [59], Astrakhantsev *et al.* [38], Harris *et al.* [35], dressed hexagon state E_α (this Letter) [Eq. (2)], Hagymási *et al.* [37], and the NLCE hexagon expansion at second order for $T = 0$ (this Letter). Estimates of the ground-state energy higher than E_α, the variational energy, can be ruled out.

The simplicity of the hard-hexagon states enables us to understand their low energy and stability, which arises from the following ingredients. The first is that the pyrochlore lattice can be decomposed into nonoverlapping hexagonal loops—the hard hexagons—which exhibit a robust finite-size gap of $\sim 0.69J$.

Second, the hexagons are connected by a quartet of bonds linking two pairs of antiferromagnetically correlated spins *symmetrically*, making the coupling *doubly frustrated* [Fig. 1(d)] [44]. This latter point is perhaps conceptually the most interesting one, as it shifts the perspective from the frustration-induced degeneracy arising on a single tetrahedron to the isolation of *unfrustrated* (nondegenerate) geometrical motifs. Third, the *kinetic* energy of local defects in this background pattern is similarly suppressed. Fourth, there are no matrix elements between different hard-hexagon coverings to any finite order in perturbation theory.

From this point forward, we discuss in detail the $S = 1/2$ hard-hexagon state on the pyrochlore lattice. Having understood its essential ingredients, we are able to apply similar constructions to the $S = 1$ pyrochlore Heisenberg model as well as Heisenberg models on the ruby [Fig. 1(b)] and checkerboard [Fig. 1(c)] lattices. In these cases, we verify that the variational energy of these states is competitive with the ground-state energy obtained by density matrix renormalization group (DMRG) methods [45–49] [Table I].

TABLE I. Ground-state energies in units of J for different models and spin lengths. The ground-state energy is calculated using second-order NLCE, DMRG, and the variational wave function Eq. (2) with optimization of the parameter α. The optimal values of α are given in Table S1 the Supplemental Material [50]. The DMRG energies for the pyrochlore lattice are from Hagymási *et al.* [37,51], while the DMRG results were obtained using ɪTensor [52].

Model	$NLCE_2$	DMRG	E_{α_0}
Pyrochlore, $S = \frac{1}{2}$	$-0.4917(5)$	$-0.490(6)$	$-0.489472(8)$
Ruby, $S = \frac{1}{2}$	$-0.492(1)$	$-0.4865(7)$	$-0.48946(5)$
Checkerboard, $S = \frac{1}{2}$	$-0.5138(2)$	$-0.5132(2)$	$-0.513442(1)$
Pyrochlore, $S = 1$	$-1.489(5)$	$-1.520(6)^*$	$-1.490(1)$
Ruby, $S = 1$	$-1.489(5)$	$-1.4764(5)$	$-1.490(1)$
Checkerboard, $S = 1$	$-1.533(2)$	$-1.532(1)$	$-1.5339(5)$

[*]Note that the $S = 1$ pyrochlore case was obtained for 48 sites, and finite-size effects are likely to underestimate the ground-state energy.

We start by covering the pyrochlore lattice with hexagons such that each site participates in exactly one hexagon. The number of ways to do this is exponentially large in the linear system size, as we discuss in more detail later. For a given covering, we then decompose the nearest-neighbor Heisenberg model into links within the hard hexagons, H_0, and the connecting terms V:

$$H = H_0 + V = J \sum_{\langle i,j \rangle \in \bigcirc} \mathbf{S}_i \cdot \mathbf{S}_j + J \sum_{\langle i,j \rangle \notin \bigcirc} \mathbf{S}_i \cdot \mathbf{S}_j. \quad (1)$$

Ground-state energy.—Crucially, the decoupled hexagon Hamiltonian H_0 exhibits a large gap $\sim 0.69J$, while the coupling V is effectively suppressed since it *symmetrically* couples pairs of neighboring—and hence *anti*ferromagnetically correlated—spins in two hexagons via the four bonds [Fig. 1(d)] of their shared tetrahedron. Moreover, the ground-state energy of H_0, $E_0 \sim -0.47J$, is already not far from the pre-existing estimates of the ground-state energy of the full pyrochlore lattice. This motivates a variational approach by which we establish a strict upper bound on the ground-state energy of Eq. (1) in the thermodynamic limit which, within error bars, competes with previous extrapolations based on estimates for small clusters [35,37,38,51].

The trial wave function is constructed by dressing the ground state of H_0, $|\Psi_0\rangle$—a simple product state. To introduce additional correlations between the hexagons and minimize the energy further, we perform imaginary-time evolution using the Hamiltonian of the tetrahedral links V, connecting the hexagons:

$$|\Psi_\alpha\rangle = e^{-\alpha V} |\Psi_0\rangle \quad (2)$$

$$\Rightarrow E_\alpha = \frac{1}{N} \frac{\langle \Psi_\alpha | H | \Psi_\alpha \rangle}{\langle \Psi_\alpha | \Psi_\alpha \rangle}. \quad (3)$$

The variational energy per site E_α, which we evaluate using an expansion in powers of α [50,53–58], exhibits a well-defined minimum at $\alpha = \alpha_0$. The expansion is fully converged around the minimum, and the truncation error of the variational energy is much smaller than the symbol size in Fig. 2(b). Importantly, the resulting minimal energy E_{α_0} (see Table I), due to its variational nature, rules out all larger estimates from previous studies [35,38], as indicated in Fig. 2(b).

We further support the stability of the hard-hexagon state by a numerical linked cluster expansion (NLCE) [60,61]. This method has proven valuable in determining thermodynamic quantities at *finite* temperature in three-dimensional lattices, including the pyrochlore lattice [59,62,63]. The algorithm is in spirit similar to a high-temperature expansion in the sense that it systematically includes larger clusters to obtain an estimate at a finite temperature. While most previous works on the pyrochlore exploit the tetrahedral structure (which is powerful at finite temperature), we generalized the expansion based on nonoverlapping hexagons [50]. Typically, the limit of convergence of a finite order expansion is clearly identified by the fact that successive orders rapidly diverge from each other to *infinity* below some temperature. This is the case for the tetrahedral expansion, as shown in Fig. 2 (orange lines). However, the situation is remarkably different for the hexagon-based expansion (blue lines in the same figure). It is clearly not converged for intermediate temperatures, $0.06J \leq T \leq 0.8J$, *but* converges again for $T \to 0$ yielding a realistic ground-state energy compatible with previous studies [35,37,38]. Strikingly, the low-temperature *convergence* is effectively obtained in the second order. This lends further credence to a particularly simple low-temperature state of weakly dressed hexagons. The success of the NLCE at $T = 0$ is reminiscent of a study of a distorted kagomé lattice [64], where a similar approach was used to support the conclusion of a dimerized ground state.

Hard-hexagon coverings and symmetry breaking.—The proposed states are nonmagnetic valence-bond crystals, whose symmetry-breaking properties are determined by the underlying coverings of the lattice by hard hexagons. The pyrochlore lattice admits an exponentially large family of hard-hexagon states, all of which take the form of long-ranged ordered planes of hexagons stacked along one of the three equivalent $\langle 001 \rangle$ directions. Taking for example the covering shown in Fig. 1(a) we can obtain a new valid covering by shifting the second plane from the bottom (composed of yellow and red hexagons) one unit to the right (i.e., along one of the $\langle 110 \rangle$ crystal directions). Assuming that all hard-hexagon coverings of the pyrochlore lattice can be constructed from such shifts, this yields a subextensive, yet exponentially large, number of coverings $N_{\text{cover}} = 3 \times 2^{4L/3}$, where L is the linear system size given as the number of cubic, 16-site unit cells. We have verified numerically [50], for finite clusters up to
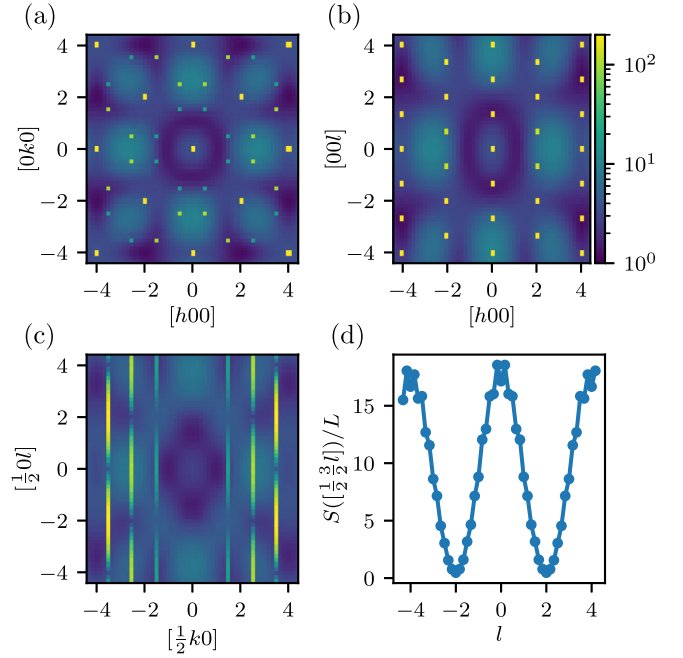

FIG. 3. Symmetry breaking of a hard-hexagon state with stacking direction [001]. We show the dimer-dimer correlation function [Eq. (4)], which, in contrast to the usual two-point correlation function, shows signatures of both the breaking of translation and rotation symmetry [Bragg peaks in panels (a),(b)] as well as of the disorder in the stacking direction [broad features in panels (c),(d)].

$L = 12$, that these are the only coverings by using an unbiased numerical optimization algorithm.

The fact that there is an infinite family of states on the pyrochlore lattice, rather than a single hard-hexagon state, is interesting for two main reasons. First, for a single such state to be stable, it is important that a finite order of perturbation theory connect no two members of the family. This is clearly the case for the stacked-layer coverings discussed above since going from one to the other requires the translation of an entire plane of hexagons. Second, this has implications for the symmetry breaking of a state randomly selected from, or averaged over, this family. Since in a valence bond solid state, two-point correlation functions decay rapidly, we instead compute a four-point correlation function which we call the dimer structure factor, or bond correlator,

$$S_{\text{dimer}}(\mathbf{q}) = \sum_{\langle ij \rangle, \langle kl \rangle} \exp\left(-i\mathbf{q} \cdot \left[\frac{1}{2}(\mathbf{r}_i + \mathbf{r}_j) - \frac{1}{2}(\mathbf{r}_k + \mathbf{r}_l)\right]\right)$$
$$\times \langle (\mathbf{S}_i \cdot \mathbf{S}_j)(\mathbf{S}_k \cdot \mathbf{S}_l) \rangle, \qquad (4)$$

for an ensemble of hard-hexagon states with [001] stacking direction obtained by the numerical optimization algorithm mentioned before. The result is shown in Fig. 3. In contrast to the "usual" spin structure factor based on a two-point correlation function, the dimer structure factor is based on a

four-point correlation function and carries signatures of the translational and rotational symmetry breaking [Bragg peaks in panels (a) and (b)] as well as the disorder in the stacking direction [broad features in panels (c) and (d)] and also the short-range correlations within the hexagons (low-intensity broad features rendered visible by the log scale).

We note that, given the nonmagnetic nature of the symmetry breaking, probes such as Raman scattering or ultrasound measurements may be useful experimentally besides neutron scattering, which can best establish the absence of long-range magnetic order.

Robustness of the gap.—Since the hard-hexagon states break only discrete symmetries, they are—if stable—generically gapped. We analyze the excitations above our family of hexagon states to asses their (local) stability. As the candidate ground states are weakly dressed product states of single-hexagon ground states, the simplest ansatz for the excited states is given analogously by weakly dressed local triplet excitations on a single hexagon. The lowest-lying excited state on a single hexagon is given by a triplet, with a gap of $\sim 0.69J$. A possibility to reduce and finally destabilize the gap would be for the localized excitations to gain *kinetic* energy. Numerically evaluating the excitation dispersion in three dimensions is difficult, and presently out of reach. Instead, we turn to an analytic approximation: namely the multiboson expansion, which is able to describe the hopping of local excitations above a given ground state, at first order in perturbation theory [50,65,66]. The results are shown in Fig. 4: remarkably, the lowest-lying triplet bands, $|t_m^-\rangle$ ($m = -1$, 0, 1) at $E \sim 0.69J$, remain completely flat, while the higher energy triplets disperse (bands labeled by $|k_n^\pm\rangle$ in Fig. 4) and are actually pushed below the excited singlet located at $E \sim 1.3J$, which also remains flat. The flatness of the bands is due to a symmetry of the hopping matrix elements V [see Eq. (1)], connecting two hexagons A and B. This is illustrated in Fig. 4(b): mirroring each hexagon *individually* across a plane running through the tetrahedron leaves the operator matrix element $V(A, B)$ invariant. This implies a selection rule for the hopping matrix element $\langle s_0, t|V|t, s_0\rangle$. Classifying all eigenstates of H_0 by the three mirror symmetries of a hexagon, it turns out that the ground state singlet $|s_0\rangle$ as well as the lowest-lying triplet $|t_m^-\rangle$ are simultaneous eigenstates of all three, but with eigenvalue $+1$ and -1 respectively. This then guarantees $\langle s_0, t_m^-|V|t_m^-, s_0\rangle = 0$ by symmetry, hence the flatness of the lowest band. By contrast, the two triplet pairs at $E \sim 1.5J$ and $E \sim 1.8J$ are *not* simultaneous eigenstates of all three mirror operations and hence are not prevented from mixing into dispersive modes. In Fig. 4(c), we show schematically a process with several high-energy virtual intermediate states, which would give the lowest-lying triplet kinetic energy. However, since this only appears at the fourth order in V, we do not expect this to lower the gap of the hard-
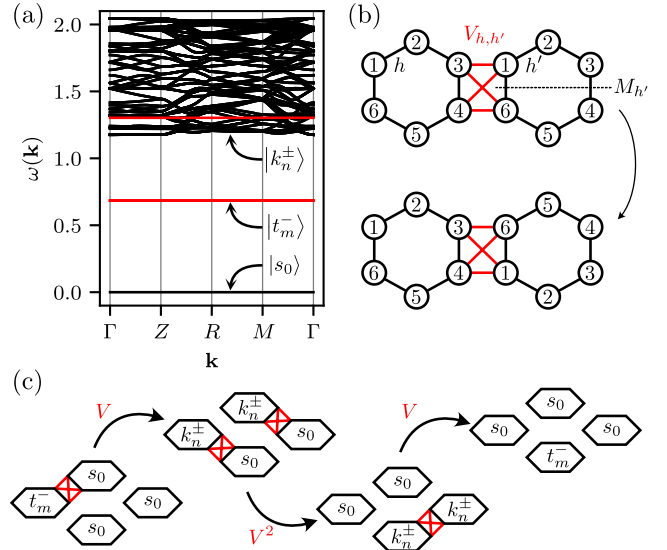

FIG. 4. (a) Dispersion of excitations above the hard-hexagon state in Fig. 1(a) up to linear order in V. (b) Coupling of hexagons and resulting local symmetry of the hopping matrix element V. Flat bands are colored in red for visibility (c) Schematic of the fourth-order hopping process by which the lowest-lying triplet $|t_m^-\rangle$ would gain kinetic energy.

hexagon state significantly. Finally, we note that the symmetry argument above does not depend on the choice of a particular tiling, but the exact shape of the dispersion of high-energy bands in Fig. 4(a) will.

To summarize our results for the pyrochlore $S = 1/2$ model, we propose an exponentially large family of valence-bond crystals based on hard-hexagon coverings as candidate ground states. A variational calculation of their energy in the thermodynamic limit is within the error bars of the best numerical estimates of the ground-state energy. The stability of these states is further supported by NLCE and by a multiboson expansion which shows that the kinetic energy of excitations is suppressed. The hard-hexagon coverings break rotation, translation, and inversion symmetries of the lattice. It is important to note that the recent numerical studies that found lattice symmetry breaking [37,38] used clusters that are incompatible with the hard-hexagon states, rendering them energetically disfavorable there.

Note that the same ingredients rendering the stability of the valance-bond state are found in other Heisenberg models, such as the two-dimensional ruby and checkerboard lattice for $S = 1/2$ and $S = 1$, cf. Fig. 1. We obtain analogous results, such as the flatness of the triplet band and a finite-size gap, in these cases. A short discussion of spin $S = 1$ [67] and broken symmetries [68–73] is given in the Supplemental Material [50].

Discussion.—Having identified a new family of energetically competitive states based on effectively decoupled close-packed motifs, we still cannot settle the question of what is the actual ground state in the pyrochlore case. On a

technical level, our study underlines the need to consider possibly very large unit cells in finite-size studies. We note that such a change in perspective was already proposed in the context of the $S = 3/2$ spinel compound $ZnCr_2O_4$ [43], where hexagonal motifs had been identified in a study of its magnetoelastic properties [74]. In this case, theoretical modeling ultimately suggested that the system is not described by independent hexagonal clusters but rather that weak further neighbor exchange can account for the salient observations [75,76]. In this work, we have demonstrated that the formation of such clusters can indeed occur, but via a different, quantum, mechanism.

The existence of potential material realizations of the pyrochlore Heisenberg antiferromagnet [77,78], and the growing capabilities of cold atom emulations [79–81], gives hope that some of these questions may eventually be settled by experiment. The presence of a significant gap to spin excitations above the hard-hexagon states would be an important signature for both thermodynamic and spectroscopy measurements if indeed the system can equilibrate into such a state at low temperatures. The presence of sharp, gapped, $S = 1$ excitations, along with the presence of lattice symmetry breaking would serve to distinguish the hard-hexagon states from competing quantum spin liquids.

However, due to the presence of such a large family of low-energy states, as well as potential additional states beyond the ansatz considered here, it may be that the physics at the temperatures reachable in the experiment is controlled not by a single ground state but by many competing ones. Further, the eventual ground-state selection in an actual material in the presence of any near degeneracies will take place via any residual deviations from an ideal Heisenberg Hamiltonian, and may require exquisitely low temperatures. Finally, hexagonal motifs have appeared in various pyrochlore settings [74–76], and the mechanisms leading to their stabilization may reinforce each other in a given material.

R. S. and B. P. contributed equally to this work.

---

[*]schaefer@pks.mpg.de
[†]placke@pks.mpg.de
[‡]benton@pks.mpg.de
[§]moessner@pks.mpg.de

[1] J. B. Marston and C. Zeng, J. Appl. Phys. **69**, 5962 (1991).
[2] R. R. P. Singh and D. A. Huse, Phys. Rev. Lett. **68**, 1766 (1992).
[3] S. Sachdev, Phys. Rev. B **45**, 12377 (1992).
[4] J. T. Chalker and J. F. G. Eastmond, Phys. Rev. B **46**, 14201 (1992).
[5] K. Yang, L. K. Warman, and S. M. Girvin, Phys. Rev. Lett. **70**, 2641 (1993).
[6] C. Waldtmann, H. U. Everts, B. Bernu, C. Lhuillier, P. Sindzingre, P. Lecheminant, and L. Pierre, Eur. Phys. J. B **2**, 501 (1998).
[7] B. H. Bernhard, B. Canals, and C. Lacroix, Phys. Rev. B **66**, 104424 (2002).
[8] R. Budnik and A. Auerbach, Phys. Rev. Lett. **93**, 187205 (2004).
[9] R. R. P. Singh and D. A. Huse, Phys. Rev. B **76**, 180407(R) (2007).
[10] M. Hermele, Y. Ran, P. A. Lee, and X.-G. Wen, Phys. Rev. B **77**, 224413 (2008).
[11] H. C. Jiang, Z. Y. Weng, and D. N. Sheng, Phys. Rev. Lett. **101**, 117203 (2008).
[12] D. Poilblanc, M. Mambrini, and D. Schwandt, Phys. Rev. B **81**, 180402(R) (2010).
[13] S. Yan, D. A. Huse, and S. R. White, Science **332**, 1173 (2011).
[14] S. Depenbrock, I. P. McCulloch, and U. Schollwöck, Phys. Rev. Lett. **109**, 067201 (2012).
[15] Y. Iqbal, F. Becca, S. Sorella, and D. Poilblanc, Phys. Rev. B **87**, 060405(R) (2013).
[16] H. J. Liao, Z. Y. Xie, J. Chen, Z. Y. Liu, H. D. Xie, R. Z. Huang, B. Normand, and T. Xiang, Phys. Rev. Lett. **118**, 137202 (2017).
[17] Y.-C. He, M. P. Zaletel, M. Oshikawa, and F. Pollmann, Phys. Rev. X **7**, 031020 (2017).
[18] A. M. Läuchli, J. Sudan, and R. Moessner, Phys. Rev. B **100**, 155142 (2019).
[19] M. J. Lawler, H.-Y. Kee, Y. B. Kim, and A. Vishwanath, Phys. Rev. Lett. **100**, 227201 (2008).
[20] M. J. Lawler, A. Paramekanti, Y. B. Kim, and L. Balents, Phys. Rev. Lett. **101**, 197202 (2008).
[21] E. J. Bergholtz, A. M. Läuchli, and R. Moessner, Phys. Rev. Lett. **105**, 237202 (2010).
[22] A. V. Chubukov and T. Jolicoeur, Phys. Rev. B **46**, 11137 (1992).
[23] R. Deutscher and H. Everts, Z. Phys. B **93**, 77 (1993).
[24] W.-J. Hu, S.-S. Gong, W. Zhu, and D. N. Sheng, Phys. Rev. B **92**, 140403(R) (2015).
[25] Z. Zhu and S. R. White, Phys. Rev. B **92**, 041105(R) (2015).
[26] Y. Iqbal, W.-J. Hu, R. Thomale, D. Poilblanc, and F. Becca, Phys. Rev. B **93**, 144411 (2016).
[27] B. Canals and C. Lacroix, Phys. Rev. Lett. **80**, 2933 (1998).
[28] B. Canals and C. Lacroix, Phys. Rev. B **61**, 1149 (2000).
[29] J. H. Kim and J. H. Han, Phys. Rev. B **78**, 180410(R) (2008).
[30] F. J. Burnell, S. Chakravarty, and S. L. Sondhi, Phys. Rev. B **79**, 144432 (2009).
[31] S.-B. Lee, S. Onoda, and L. Balents, Phys. Rev. B **86**, 104412 (2012).

[32] Y. Iqbal, T. Müller, P. Ghosh, M. J. P. Gingras, H. O. Jeschke, S. Rachel, J. Reuther, and R. Thomale, Phys. Rev. X **9**, 011005 (2019).

[33] H. Tsunetsugu, J. Phys. Soc. Jpn. **70**, 640 (2001).

[34] M. Isoda and S. Mori, J. Phys. Soc. Jpn. **67**, 4022 (1998).

[35] A. B. Harris, A. J. Berlinsky, and C. Bruder, J. Appl. Phys. **69**, 5200 (1991).

[36] E. Berg, E. Altman, and A. Auerbach, Phys. Rev. Lett. **90**, 147204 (2003).

[37] I. Hagymási, R. Schäfer, R. Moessner, and D. J. Luitz, Phys. Rev. Lett. **126**, 117204 (2021).

[38] N. Astrakhantsev, T. Westerhout, A. Tiwari, K. Choo, A. Chen, M. H. Fischer, G. Carleo, and T. Neupert, Phys. Rev. X **11**, 041021 (2021).

[39] M. Hering, V. Noculak, F. Ferrari, Y. Iqbal, and J. Reuther, Phys. Rev. B **105**, 054426 (2022).

[40] O. Benton, L. D. C. Jaubert, R. R. P. Singh, J. Oitmaa, and N. Shannon, Phys. Rev. Lett. **121**, 067201 (2018).

[41] I. Hagymási, R. Schäfer, R. Moessner, and D. J. Luitz, Phys. Rev. B **106**, L060411 (2022).

[42] J. Schnack, J. Schulenburg, and J. Richter, Phys. Rev. B **98**, 094423 (2018).

[43] S.-H. Lee, C. Broholm, W. Ratcliff, G. Gasparovic, Q. Huang, T. H. Kim, and S.-W. Cheong, Nature (London) **418**, 856 (2002).

[44] A. A. Nersesyan and A. M. Tsvelik, Phys. Rev. B **67**, 024422 (2003).

[45] F. Verstraete, J. J. García-Ripoll, and J. I. Cirac, Phys. Rev. Lett. **93**, 207204 (2004).

[46] U. Schollwöck, Rev. Mod. Phys. **77**, 259 (2005).

[47] A. E. Feiguin and S. R. White, Phys. Rev. B **72**, 220401(R) (2005).

[48] U. Schollwöck, Ann. Phys. (Amsterdam) **326**, 96 (2011).

[49] E. Stoudenmire and S. R. White, Annu. Rev. Condens. Matter Phys. **3**, 111 (2012).

[50] See Supplemental Material at http://link.aps.org/supplemental/10.1103/PhysRevLett.131.096702 for a detailed description of all calculations and analysis performed in this letter.

[51] I. Hagymási, V. Noculak, and J. Reuther, Phys. Rev. B **106**, 235137 (2022).

[52] M. Fishman, S. R. White, and E. M. Stoudenmire, SciPost Phys. Codebases 4 (2022).

[53] H. D. Ursell, Math. Proc. Cambridge Philos. Soc. **23**, 685 (1927).

[54] K. A. Brueckner, Phys. Rev. **97**, 1353 (1955).

[55] J. Goldstone, Proc. R. Soc. A **239**, 267 (1957).

[56] J. K. Percus, Commun. Math. Phys. **40**, 283 (1975).

[57] S. B. Shlosman, Commun. Math. Phys. **102**, 679 (1986).

[58] R. Mattuck, *A Guide to Feynman Diagrams in the Many-Body Problem*, Dover Books on Physics Series (Dover Publications, New York, 1992).

[59] R. Schäfer, I. Hagymási, R. Moessner, and D. J. Luitz, Phys. Rev. B **102**, 054408 (2020).

[60] B. Tang, E. Khatami, and M. Rigol, Comput. Phys. Commun. **184**, 557 (2013).

[61] R. Schäfer, Magnetic frustration in three dimensions (2022), https://nbn-resolving.org/urn:nbn:de:bsz:14-qucosa2-829375.

[62] R. Applegate, N. R. Hayre, R. R. P. Singh, T. Lin, A. G. R. Day, and M. J. P. Gingras, Phys. Rev. Lett. **109**, 097205 (2012).

[63] R. R. P. Singh and J. Oitmaa, Phys. Rev. B **85**, 144414 (2012).

[64] E. Khatami, R. R. P. Singh, and M. Rigol, Phys. Rev. B **84**, 224411 (2011).

[65] S. Sachdev and R. N. Bhatt, Phys. Rev. B **41**, 9323 (1990).

[66] J. Romhányi and K. Penc, Phys. Rev. B **86**, 174428 (2012).

[67] F. D. M. Haldane, Phys. Rev. Lett. **50**, 1153 (1983).

[68] B. Sriram Shastry and B. Sutherland, Physica (Amsterdam) **108B+C**, 1069 (1981).

[69] P. Sindzingre, J.-B. Fouet, and C. Lhuillier, Phys. Rev. B **66**, 174424 (2002).

[70] J.-B. Fouet, M. Mambrini, P. Sindzingre, and C. Lhuillier, Phys. Rev. B **67**, 054411 (2003).

[71] W. Brenig and A. Honecker, Phys. Rev. B **65**, 140407(R) (2002).

[72] Y.-H. Chan, Y.-J. Han, and L.-M. Duan, Phys. Rev. B **84**, 224407 (2011).

[73] R. F. Bishop, P. H. Y. Li, D. J. J. Farnell, J. Richter, and C. E. Campbell, Phys. Rev. B **85**, 205122 (2012).

[74] O. Tchernyshyov, R. Moessner, and S. L. Sondhi, Phys. Rev. Lett. **88**, 067203 (2002).

[75] P. H. Conlon and J. T. Chalker, Phys. Rev. B **81**, 224413 (2010).

[76] T. Yavors'Kii, T. Fennell, M. J. P. Gingras, and S. T. Bramwell, Phys. Rev. Lett. **101**, 037204 (2008).

[77] L. Clark, G. J. Nilsen, E. Kermarrec, G. Ehlers, K. S. Knight, A. Harrison, J. P. Attfield, and B. D. Gaulin, Phys. Rev. Lett. **113**, 117201 (2014).

[78] S. Zhang, H. J. Changlani, K. W. Plumb, O. Tchernyshyov, and R. Moessner, Phys. Rev. Lett. **122**, 167203 (2019).

[79] D.-W. Zhang, Y.-Q. Zhu, Y. X. Zhao, H. Yan, and S.-L. Zhu, Adv. Phys. **67**, 253 (2018).

[80] A. Browaeys and T. Lahaye, Nat. Phys. **16**, 132 (2020).

[81] G. Semeghini, H. Levine, A. Keesling, S. Ebadi, T. T. Wang, D. Bluvstein, R. Verresen, H. Pichler, M. Kalinowski, R. Samajdar, A. Omran, S. Sachdev, A. Vishwanath, M. Greiner, V. Vuletić, and M. D. Lukin, Science **374**, 1242 (2021).

[82] M. Yang and S. R. White, Phys. Rev. B **102**, 094315 (2020).

Correction: The colors given in the Fig. 2 caption to describe the curves in panel (a) were interchanged and have been fixed.